Silanization by Room Temperature Chemical Vapor Deposition and Controlled Roughness for Wettability Modification of Microfluidic and Microfabrication Substrates

Patrcia Canané
patricia.canane@tecnico.ulisboa.pt

Instituto Superior Técnico, Lisboa, Portugal

August 2019

Abstract

Microfluidics provides a portable, cost-effective, rapid and low consumption alternative to the typical laboratory instruments used for biological detection. Microfluidic devices benefit from microfabrication techniques, which allow the design of complex nano/micro-scale structures. However, high surface to volume ratio generates problems of biofouling, unwanted cell behaviour and surface-surface adhesion, jeopardizing the efficiency of microfluidic and microfabrication techniques. Chemical or physical surface wettability modification (SWM) is an expedite method to tailor adhesion forces. In this work, silanization with HMDS, FDTS and APTES by Room Temperature Chemical Vapor Deposition (RT-CVD) was applied in samples of silicon, glass, PDMS (polydimethylsiloxane), SU-8 photoresist and thin films (of gold, silicon dioxide and alumina). Deterministic Roughness was implemented in silicon dioxide thin films ($CA_{t0} \simeq 80°$), by crafting square structures on the substrate. SWM was assessed by measurements of liquid-solid contact angle (CA). Hydroxyl (-OH) containing surfaces ($CA_{t0} < 20°$), subjected to RT-CVD exhibited an increase in CA ($70° < CA < 100°$) due to establishment of silane-surface covalent bonds and exposure of non-polar groups. Functionalization of gold films ($CA_{t0} \simeq 80°$) with FDTS ($CA \simeq 100°$) and APTES ($CA \simeq 40°$) was also observed. Functionalization of PDMS substrates and SU-8 was achieved, but the hydrophobic behaviour persisted. XPS analysis of alumina thin films exposed to APTES indicated the presence of hydrogen-bonded APTES molecules. Implementation of square structures of varied size (1-5 μm) and spacing (2-5 μm) lead to an increase in CA up to 35%.

Keywords: Surface tailoring, Room Temperature Chemical Vapor Deposition, Surface Roughness, Contact angle.

1. Introduction

Microfluidic devices have gained great academic and industrial interest due to their portability, cost-effectiveness, reduced reagent consumption and time of analysis. These devices provide a precise and controlled environment for studies of cell growth and proliferation, being a expedient alternative to the conventional biological laboratory methods [1], benefiting from microfabrication techniques for design of complex structures. However, due to their high surface to volume ratio consequent of nano/micro-scale processing, surface tension, adhesion and cohesion forces have a high impact in the efficiency of the system and fabrication steps, where surface-surface and bioanalite-surface adhesion is of extreme importance. As an example, PDMS (polydimethylsiloxane) is a very commonly used polymer in the microfabrication of microfluidic channels, due to its biocompatibility, permeability to gases, low-cost and optical transparency. Since the material is hydrophobic (or repels water), water and water-based solutions show difficulty passing through the channels, being necessary a more powerful pump to reach the desired flow, increasing the device cost [2]. Also, cells and enzymes show great adhesion to hydrophobic materials, exhibiting different morphology and behavior consequent of surface topography and chemical composition [3, 4].

Surface wettability is understood as the consequent phenomena of the balance between adhesion (liquid-surface) and cohesion (liquid-liquid) forces [5]. If liquid-substrate adhesion forces are stronger than the cohesion forces, the surface shows high wettability ($CA \ll 90°$, hydrophilic, fluidophilic or lyophilic surface), but if cohesion forces surpass adhesion forces, a hydrophobic behavior is observed ($CA \gg 90°$, hydrophobic, fluidophobic or lyophobic surface). The influence of these forces can be

perceived by measurements of contact angle (CA) formed between droplets of liquid and the surface. By tailoring the wettability of the surface, adhesion and cohesion can be controlled, enhancing the efficiency of the analysis at the micro-scale. Therefore, Surface Wettability Modification (SWM) appears as a useful tool to alter surface wettability and control forces at the biomolecule-material or fluid-material level. SWM, already a subject of study for biological and biomedical applications [6, 7], can be achieved by altering the superficial chemical layer or roughness of the material substrate, being the latter stochastic or deterministic. Considering only the chemical exposed groups of the material, the wettability can be evaluated by the Young model (eq. 1), which only considers interfacial forces, being γ_{lv} the liquid-vapor interface energy,γ_{sv} the interfacial energy between solid surface and vapor and γ_{sl} the solid-liquid interfacial energy.

$$cos(\theta_Y) = \frac{\gamma_{sv} - \gamma_{sl}}{\gamma_{lv}} \tag{1}$$

If the topography of the surface is being altered, the consequent wettability modification can be explained by the Wenzel (eq. 2) or Cassie-Baxter models (eq. 3), where θ_W is the Wenzel contact angle, r is the roughness value of the solid, θ_C is the Cassie-Baxter contact angle, f is the fraction of the solid that is wet, (1-f) is the fraction of air gasps and θ_X is the CA on the gas in the gaps.

$$cos(\theta_W) = rcos(\theta_Y) \tag{2}$$

$$cos(\theta_C) = fcos(\theta_Y) + (1-f)cos(\theta_X) \tag{3}$$

Chemical functionalization resides on the modification of the available chemical groups on the surfaces, by exposure to adequate chemical agents. Chemical SWM highly depends on the polarity of the surface. Polar groups, such as hydroxyl (-OH), are responsible for a high surface energy or wettability, while non-polar groups, such as hydrocarbons, decrease surface energy. Silanes are commonly used in chemical SWM, especially in hydrophilic surfaces, where a covalent molecular attachment is expected. Silanes are amphiphilic functional molecules with the general formula X-$(CH_2)_n$-$SiR_n(OR)_{3-n}$ where X represents the functional group, $(CH_2)_n$ the flexible spacer and $Si(OR)_{3-n}$ the anchor groups that can react with the exposed groups on the substrate. If the adsorption of silane molecules occurs, a self-assembled monolayer (SAM) of amphiphilic molecules is formed on the surface [8]. HMDS (hexamethyldisilazane), FDTS (perfluorodecyltrichlorosilane) and APTES ((3-aminopropyl)triethoxysilane) are the most used chemical agents for SWM for non-biological and biological applications, due to their high affinity to oxidized surfaces and high hydrophobic potential [9, 10]. HMDS is a secondary amine, with the chemical formula $HN[Si(CH_3)_3]_2$, that reacts with hydroxyl surfaces, leaving methyl (-CH_3) groups bonded to the surface [11]. FDTS ($CF_3(CF_2)_7(CH_2)_2(SiCl_3)$) is a more complex molecule, due to the number of final atoms on the head group (in this case, three chlorine atoms). It is not guaranteed that all chlorine atoms react with the oxidized surface, leading to different molecule orientations (horizontal or vertical). The orientation of the molecule after adsorption to the surface is a very important parameter, as the type of chemical group exposed (CF_2 or CF_3 groups) impact surface wettability [12]. APTES is a very complex silane, due to the several possible reactions with the surface. Reaction of the three head groups of APTES (ethoxy groups) with oxidized surfaces requires a step of hydrolysis, which occurs in the presence of trace volumes of water. However, APTES is a hygroscopic agent, which means that the hydrolysis step is very difficult to control, as it is sensitive to water present in the surface and surrounding air. Plus, the amine group of APTES molecules can establish hydrogen bonds with hydroxyl groups, exposing the ethoxy groups away from the surface [13].

The exposure of surfaces to silane agents can be performed by Room Temperature Chemical Vapor Deposition (RT-CVD). RT-CVD is a simple, cost-effective technique which requires small volumes of reagents ($<$ 1 mL), has high deposition rates and does not transport any impurities along the vapor phase, possibly present in the liquid phase. In RT-CVD, vapor-molecules of the chemical modifying agent are deposited on the surface, under vacuum and room temperature conditions. The reagent molecules react with the chemical exposed groups of the surface, consequently exhibiting groups with higher or lower polarity compared to the untreated surface, tailoring surface wettability. Moreover, SWM by surface topography modification is being explored nowadays to successfully implement stochastic and deterministic roughness, including attachment of nanoparticles, design of specific patterns or usage of plasma etching [14, 15]. Processes of photolitography are an adequate method to implement deterministic roughness, due to the control of the type of structures present on the surface (e.g. square patterns, spikes) and their dimensions (size, spacing, height) [16].

In this work, two methods of SWM were studied. The first method consisted on RT-CVD, where vapor-phases of HMDS, FDTS and APTES silanes were used to chemically modify surfaces commonly used in microfluidics for biological assays: hydrophilic samples (CA $\ll 90°$) of silicon, glass, thin films of gold, alumina (Al_2O_3) and silicon

dioxide(SiO_2), hydrophobic substrates (CA $\gg 90°$) of PDMS (polydimethylsiloxane) and SU-8 photoresist polymers. The second method consisted on the implementation of deterministic roughness by designing square structures of 1 to 5 μm spaced by 2 to 5 μm in silicon dioxide substrates, using a photolithography process.

2. Materials and Methods

2.1. *Materials*

Silicon samples (single side polished Si, mechanical grade, 0.65 mm thick, University Wafer), hard flat samples of glass microscope slides (76 x 26 x 1 mm thick, Normax), SU-8 2005 photoresist coatings (5 μm thickness, permanent epoxy negative photoresist, Microchem) and PDMS membranes (10:1, 0.5 mm thickness, SYLGARD 184 silicone elastomer, Dow Corning) were exposed to HMDS vapor (hexamethyldisilazane ($HN[Si(CH\_3)_3]_2$, 161.40 $gmol^{-1}$, 96.0 % , TCI) and FDTS vapor (perfluorodecyltrichlorosilane, $(CF_3(CF_2)_7(CH_2)_2[SiCl_3]$, 581.56 $gmol^{-1}$, 97.0 %, Alfa Aesar) at room temperature. Thin films of gold (500 thick, 18 x 10 mm), silicon dioxide (1000 thick, 25.4 x 25.4 mm) and alumina (1000 thick, 22 x 12 mm) samples were exposed to HMDS, FDTS and APTES vapor ((3-aminopropyl)triethoxysilane, $NH_2(CH_2)_3Si(OCH_2CH_3)_3$, 221.37 $gmol^{-1}$, 99.0 %, Acros Organics), in the same working conditions.

2.2. *Sample Preparation*

Silicon and **glass** substrates were first washed with Alconox anionic detergent in a ultrasound bath for 3h, rinsed with isopropanol (IPA, > 99.8 %, Labchem), deionised (DI) water and blow dried. **PDMS** membranes were fabricated by mixing 3 dimethyl siloxane and 184 silicone elastomer (cross linking agent) in a ratio of 10:1 and put on a vacuum desiccator for 1 hour (1-800-4Bel-Art, Bel-Art Products) to remove any bubbles formed during the mixing step. Finally, a cure step was performed at 70 °C for 1 hour (Memmert GmbH + Co. KG 100-800 oven). A homogeneous coating of **SU-8 2005** of 5 μm thick was obtained on silicon pieces previously dehydrated, by a 2-step spin coating process (step 1: 500 rpm for 10 s at 100 $rpm.s^{-1}$, step 2: 3056 rpm for 30 s at 300 $rpm.s^{-1}$; Modular spin coater ws-650-23NPP, Laurell Technologies Inc.) followed by a soft baking step on a hot plate (95 °C for 2 min, SD160 hotplate, Stuart). Later, a step of UV light exposure (17 s, 5.95 $W.cm^{-2}$, UH-H 254, UV Light Technology LTD; black filter: 320-405 nm) of the SU-8 2005 was performed, followed by a second soft bake step (95 °C for 3 min). Finally, the substrate was left to cool down to room temperature ($\sim$ 22°C). To avoid any surface contamination, all steps were executed inside a laminar flow hood (Faster-BSC-EN). **Gold thin films** of 500 Åwere deposited on silicon surfaces by Ion Beam Deposition and stored in petri dishes under ambient conditions. Due to the poor adhesion of gold to silicon surfaces, a prior deposition of a chromium thin film is necessary (Alcatel, base pressure of 7.0x10^{-7} torr, Cr: 2.89 mtorr, 20 sccm, 20 W_{RF}; Au: 2.89 mtorr, 20 sccm, 20W_{RF}, 9 W, 160 Vbias) For surface wettability assays, gold thin film pieces were rinsed with isopropanol (> 99.8 % , Labchem), DI water and blow dried. **Aluminum oxide thin films** with a thickness of 1000 Åwere deposited onto silicon surfaces by Radio Frequency Sputtering (UHV II, base pressure of 7.5x10^{-7} torr, applied power of 200 W_{rf}, 543 Hz, argon flux of 43.9 sccm, deposition pressure of 4.6 mtorr). These films were used for SWM assays immediately after deposition, so no cleaning step was performed. **Silicon dioxide thin films** of 1000 Åwere grown on glass surfaces (Corning Eagle XG, 0.7 mm thick) by Magnetron Sputtering (Alcatel, applied power 140W_{RF}, argon flux of 20 sccm, 4 rpm, deposition pressure of 1.80 mTorr, base pressure in the order of 10^{-7} torr, deposition rate of 0.44 Å/s) and stored in petri dishes under ambient conditions, until SWM assays.

2.3. *Surface Wettability Modification by RT-CVD*

Substrates were exposed to a volume of 6 μL of HMDS, FDTS or APTES vapor on a vacuum desiccator (Bel-Art Products) for 2, 10, 20, 30 and 50 minutes at ambient temperature (22 °C) and pressure -078 ± 0.09 atm (R5 rotary vane vacuum pump, Busch).

2.4. *Surface Roughness Modification*

Silicon dioxide thin films were prepared as mentioned in section 2.2. Roughness of these films was physically modified by a photolithography process, where square structures of 1 to 5 μm spaced by 2 to 5 μm and height of $\simeq$ 915,8 $\mathring{A}$ were obtained. The photolitography process included: coating of the surface with a 1.5 μm thick layer of photoresist (spin-coating step at 500 rpm for 10 s, followed by a spin at 2500 rpm for 30 sec and a soft bake step at 87 °C for 60 sec), exposure to UV light (energy: 55% , power: 100 mW, focus: -10, time: 20 min, Heidelberg Instruments Direct Laser Lithography System) and photoresist development (baking step at 110 °C for 60 sec, followed by a cooling step for 30 sec and exposure to the developer TMA238WA for 60 sec). The substrates were etched by reactive ion etching (LAM Research 450, applied power of 100 W, CF_4 flux of 100 sccm, water flux of 200 sccm, base pressure of 140 mTorrs, etching rate of 9.1585 $\mathring{A}.s^{-1}$) and individualized (Disco Dad-321 Dicing Saw) into 6 x 15 mm pieces, were each square pattern was present. PR was removed by immersing the substrates in Microstrip 3001 (Fujifilm) for 1h

at 65 °C, rinsed with IPA, DI water and blow dried.

2.5. *Sample Characterization*

2.5.1 Contact Angle Measurements

For contact angle evaluation, a controllable syringe pump (NE 4000, New Era) with a 1 mL syringe (CODAN) and polyethylene tubbing BTPE-90 (863.3 μm inner diameter, Instech Lab) were used to dispense droplets of DI water and phosphate-buffered saline (PBS) solution onto the surfaces: 6 μL droplets for Si, glass, PDMS elastomer and SU-8 2005 photoresist; 3 μL drops for thin films.

Endurance of silanization with HMDS and FDTS on silicon surfaces was also analyzed, through CA measurements over 65 hours, after 50 min of RT-CVD. Wettability of structured surfaces was assessed with CA measurements of 3 μL droplets of DI water. Control measurements of CA (CA_{t0}, $CA_{L=0}$ and $CA_{d=0}$) were also performed in clean, unmodified surfaces. The different combinations of experimental conditions (surface - liquid - chemical agent - exposure time and surface - liquid - square pattern) were repeated three times. For drop dispense, the substrates were placed in a control chamber, to reduce surface contamination. Pictures of droplets were taken with a CMOS camera (5.1 m pixel size, 12 Mpixel) coupling a macro lens with 0.33 maximum magnification, for CA analysis. A light source was placed behind the control chamber, to ensure high contrast in the pictures. Pictures of droplets on surfaces chemically functionalized were recorded under ambient conditions within 5 min after RT-CVD exposure. CA analysis was performed using Image J software with Low-bond axisymmetric drop shape analysis (LBADSA) plugin [17].

2.5.2 X-ray photoelectron spectroscopy (XPS) analysis

The elemental analysis of clean, non-exposed and modified samples of alumina thin films was performed in Kratos XSAM800 apparatus with Mg Kα radiation (hν = 1253.6 eV), to confirm the presence of silane molecules on the surface, the type of silane-surface bond established and consequent molecular orientation.

3. Results and Discussion

In this section, the results obtained by Room Temperature Chemical Vapor Deposition of HMDS, FDTS and APTES silanes on several microfluidic materials and implementation of deterministic roughness on silicon dioxide thin films are discussed. Only CA measurements of DI water droplets consequent of RT-CVD will be presented, given that values obtained for PBS droplets are identical (fig. 1).

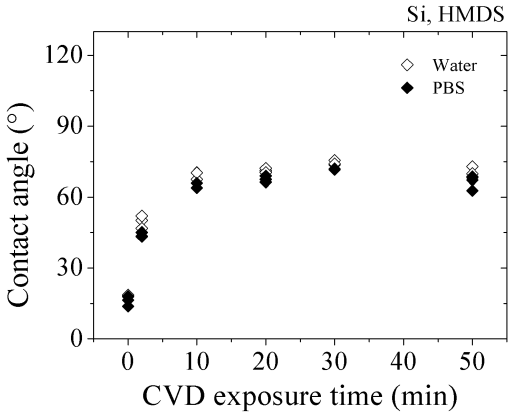

Figure 1: CA measurements of DI water droplets and PBS droplets on Si surfaces previously exposed to HMDS.

3.1. *SWM of Silicon, Glass and Polymer Surfaces*

Exposure of hydroxyl-containing surfaces (**silicon** and **glass**, CA $< 20°$) to a vapor-phase of HMDS lead to a decrease in surface wettability or surface interfacial energy ($CA_{glass,HMDS} \simeq 65°$ and $CA_{Si,HMDS} \simeq 70°$), reaching a plateau after 30 min of RT-CVD (fig. 2).

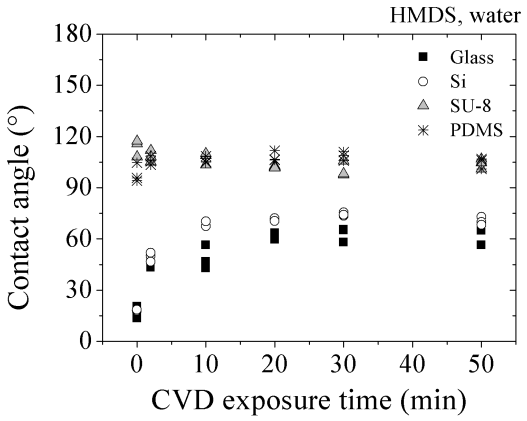

Figure 2: Measurements of CA of DI water droplets on silicon, glass, PDMS and SU-8 substrates, after RT-CVD with HMDS.

The change in wettability observed after silanization of Si and glass substrates is a consequence of the chemical groups exposed on the surface after covalent reaction with HMDS molecules. Si atoms present on HMDS molecules react with the oxygen atoms of hydroxyl groups -(OH), establishing siloxane (Si-O-Si) bonds with the surface. Consequently, methyl groups (-CH_3) remain attached to the surface, decreasing surface wettability due to their non-polar character [18].

Chemical exposure of **SU-8 photoresist** substrates ($CA_{t0} \simeq 120°$) resulted in a decrease in CA measurements ($CA_{t10} \simeq 100°$) which persisted for

higher exposure times. This behavior can be explained by a reaction between secondary amines and epoxy groups present in SU-8 surfaces. The free pair of electrons from the nitrogen atom of HMDS attacks the methylene (-CH_2) groups of epoxy, generating hydroxyl groups, which increased the number of liquid-surface hydrogen-bonds. However, these were not sufficient to surpass the hydrophobic potential of the remaining molecule, maintaining a low wettability.

Untreated **PDMS** substrates show an initial hydrophobic behaviour ($CA_{t0} \simeq 108°$), consequent of the exposure of methyl (-CH3) groups on the surface. Reactiveness of these groups depends on the adjacent substitutes present in the molecule. In the case of PDMS, methyl groups are very non-reactive and the nucleophile attack from HMDS does not happen, which justifies the negligible variation of CA measurements observed. Nonetheless, RT-CVD with HMDS for wettability modification of PDMS surfaces may be employed to prevent adhesion between PMDS masters and PMDS molds, commonly used in microfabrication [19].

As HMDS, FDTS forms self-assembled monolayers upon reaction with the superficial chemical layer of substrates, in which trichlorosilane functional groups (-$SiCl_3$) of FDTS covalently react with oxide surfaces, releasing hydrochloric acid (HCl). The increase observed in CA measurements on **glass** and **silicon** samples ($CA \simeq 70°$) is attributed to the heavily fluorinated tails of FDTS molecules (fig. 3).

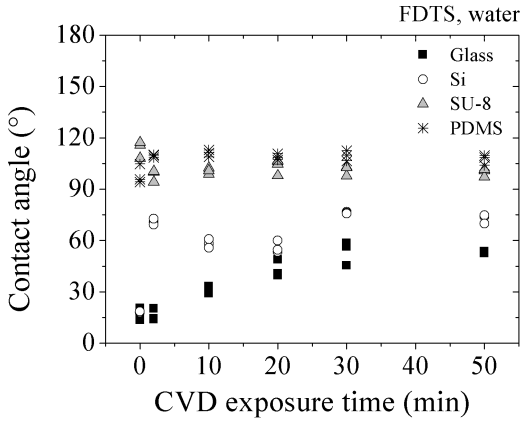

Figure 3: Measurements of CA of DI water droplets on silicon, glass, PDMS and SU-8 substrates, after RT-CVD with FDTS.

The surface coverage with a SAM of FDTS molecules seems to be reached sooner for silicon samples (saturation around 20 min of exposure to FDTS) then for glass (saturation around 50 min of exposure to FDTS). This behavior might be explained by the presence of boron ions on the glass structure, which reduce the kinetics of FDTS with hydroxyl groups present at the surface [20]. Chemical activation of **SU-8** substrates with FDTS lead to a slight increase in surface interfacial energy ($CA_{t2} \simeq 100°$), which might be explained by a chemical reaction that occurs in the polymerization phase. The polymerization of SU-8 monomers after post-exposure bake opens the epoxide group, generating hydroxyl groups available to react with FDTS free molecules [21]. Although FDTS shows a high hydrophobic potential, SWM depends on the wettable nature of the new chemical moieties attached on the surface, thus comparing to the wettable behavior of SU-8, FDTS has a higher wettable nature.

Exposure of **PDMS** substrates to FDTS lead to a decrease in surface wettability (CA increased from $\simeq 100°$ to $\simeq 112°$). Although no reaction occurs between PDMS and FDTS molecules, the presence of FDTS molecules on the surface in a horizontal conformation leads to the exposure of difluoromethylene (-CF_2) groups, which have a higher hydrophobic potential than methyl (-CH_3) groups exposed on PDMS substrates [18].

The stability of HMDS and FDTS formed SAM is an important parameter in SWM strategies in the fabrication and usage of microfluidic devices for biological applications. CA values on silicon pieces exposed to HMDS and FDTS for 50 min by RT-CVD were obtained over time. The results displayed in fig. 4 of CA measurements of DI water droplets on Si samples exposed to HMDS for 50 min do not show significant variation over time ($CA_{HMDS,water} = 63° \pm 5°$) whereas FDTS modified surfaces reveal a slight variability ($CA_{FDTS,water} = 71° \pm 9°$).

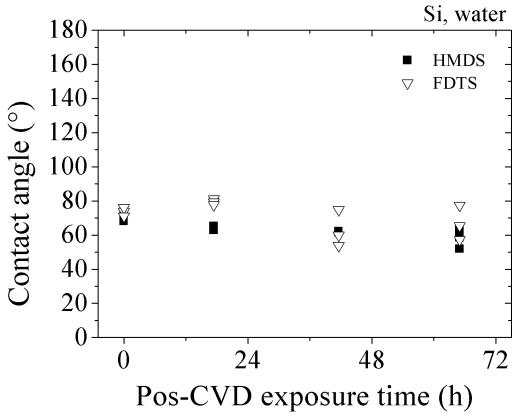

Figure 4: Measurements of CA of DI water droplets on silicon samples exposed to HMDS for 50 min by RT-CVD. CA measurements seem to persist for at least 65 hours.

This variability in CA may result from the formation of a lower-quality SAM on the silicon surface consequent of the absence of a significant volume of water inside the desiccator. Despite the high re-

activity of trichlorosilane groups of FDTS with hydroxyl groups, it is unlikely that all Si-Cl moieties react with the -OH groups present at the surface. Because of this, the FDTS SAM formed is constituted by molecules that are not covalently bonded to the surface, resulting in a low coverage or low-quality SAM [22].

Overall, the chemical modification of silicon surfaces with HMDS and FDTS is seen to be stable and persist for at least 65 hours (CA $\simeq 70°$) after RT-CVD.

3.2. *SWM of Thin Films Substrates*

Measurements of CA of DI water drops (fig. 5) on thin films show that SWM with HMDS vapor was more efficient for highly hydrophilic surfaces (**alumina** thin films) as CA increased from $\simeq 16°$ to $\simeq 100°$, reaching a plateau after 30 min of exposure.

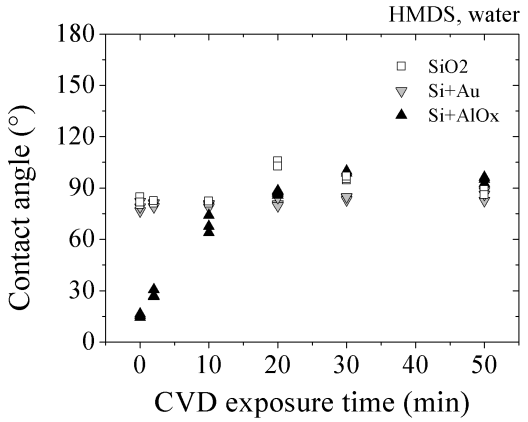

Figure 5: Measurements of CA of DI water droplets on thin films (1000 $\mathring{A}$) of gold, alumina and silicon dioxide after deposition of vapor-phase HMDS by RT-CVD.

A decrease of surface energy for Al_2O_3 films was expected, as the surface characteristically displays a layer of hydroxyl groups. These results are consistent with the ones obtained by Tasaltin *et al* [23], where the functionalization of a non-porous alumina film with HMDS by CVD for 4 hours and 100°C lead to an increase of CA to 100°, due to the presence of methyl groups on the surface following chemical exposure. Unlike alumina films, **silicon dioxide** thin films showed an initial hydrophobic tendency ($CA_{SiO2;t0} \simeq 80°$), which indicates that less hydroxyl groups were available for covalent attachment of HMDS molecules, possibly due to carbonaceous contamination consequent of film aging [24]. A significant increase in CA of SiO_2 films is only observed after 20 min of activation (CA $\simeq 100°$), which is assumed to be a result of exposure of methyl groups at the surface consequent of chemical reaction with HMDS molecules.

Research regarding silanization of **gold** thin films or gold nanoparticles with alkanethiolates is highly explored in the literature. However, the same can not be said about chemical functionalization with HMDS or FDTS silanes. Functionalization of gold thin films with HMDS or FDTS silanes may be pertinent to improve microfabrication techniques or to study cell behavior secondary to exposure to methylated and fluorinated surfaces.

Regarding gold surface wettability, an atomic-level clean surface of gold should have a practically null contact angle (CA $\simeq 0°$) [25]. However, gold surfaces quickly gather carbonaceous contamination when exposed to air or even cleaner environments , such as mercury vacuum (10^{-4} mm) or clean argon atmosphere (1 atm), increasing the surface contact angle ($70° < CA < 80°$) [26]. In this work, gold thin films exhibited an initial hydrophobic tendency ($CA_{t0} \simeq 80°$). Additionally, gold thin films have no hydroxyl groups exposed as a result of its non-oxidative character, hence will not react with HMDS. The values of CA obtained might be explained by the similarity in surface energy between the carbonaceous contamination of gold thin films surfaces and the predominant presence of hydrocarbon groups on HMDS molecules deposited on the surface.

In fig. 6, the high hydrophobic potential of FDTS is clearly visible after exposure of Al_2O_3 thin films by RT-CVD, where CA values of DI water droplets increased by 83.2% after 10 min of chemical activation which endured over time. The exposure of silicon dioxide and gold thin films to FDTS lead to an increase in CA measurements of 31% after 10 min and of 25% after 2 min, respectively.

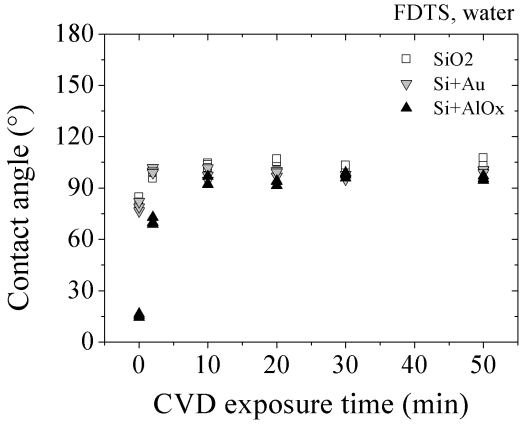

Figure 6: Measurements of CA of DI water droplets on thin films (1000 $\mathring{A}$) of gold, alumina and silicon dioxide after deposition of vapor-phase FDTS by RT-CVD.

The establishment of a covalent bond between FDTS molecules and available hydroxyl groups on

the surface of **alumina** and **silicon dioxide** thin films occurs, resulting in the exposure of FDTS fluorine groups (CF_n). Although some carbonaceous contamination might be present in SiO_2 films, the hydrophobic potential of FDTS is higher than the potential of the carbon elements, which justifies the increase observed in CA measurements.

As for **gold** thin films, no reaction between FDTS molecules and this material is described in the literature. It is proposed that FDTS molecules rest on top of gold thin films, exposing mostly difluoromethylene ($-CF_2$) groups which have a higher hydrophobic character than any carbonaceous contamination present in the films. Since activation of gold thin films with FDTS silane lead to practically the same CA threshold value as for SiO_2 and Al_2O_3 thin films, it is assumed that some FDTS molecules, after reaction with the -OH groups present in silicon dioxide and alumina surfaces might be in an horizontal orientation, exposing mainly their -CF2 groups [18]. This assumption is supported by the fact that it is improbable that all head groups of FDTS react with the disperse -OH groups exposed at the surface without a prior hydrolysis of the FDTS molecules.

Results obtained for DI water droplets (fig. 7) consequent of surface exposure to APTES show that higher CA values were obtained for **SiO_2** surfaces (CA increased from $\simeq 80°$ to $\simeq 105°$), changing from an initial hydrophobic tendency to a truly hydrophobic character, which was maintained with the increase of exposure time.

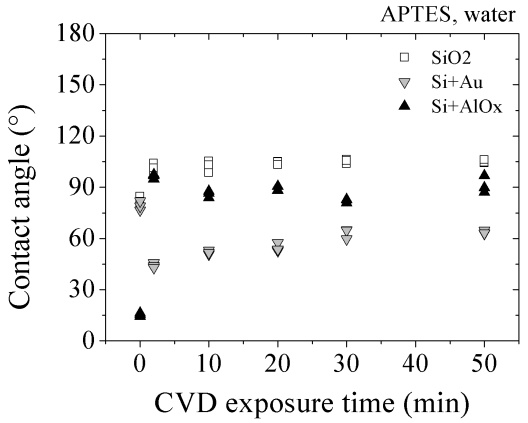

Figure 7: Measurements of CA of DI water droplets on thin films (1000 $\mathring{A}$) of gold, alumina and silicon dioxide after deposition of vapor-phase APTES by RT-CVD.

Ethoxy groups present on APTES molecules are expected to react with hydroxyl groups present on the surface, leading to the exposure of amine groups. However, APTES molecules may adopt different orientations depending on the number of ethoxy groups that covalently bond with the surface. Plus, amine groups can establish hydrogen-bonds with existing hydroxyl groups, leading to the exposure of ethoxy groups. Kyaw, H. and coworkers [27] studied the liquid-phase functionalization of glass samples with APTES and the resultant effect in self organization of gold nanoparticles. The authors observed that a CA value of 40° corresponded to the major exposure of amine groups on glass samples following functionalization, while CA>40° was consequent of the exposure of ethoxy groups at the surface.

This lead to the conclusion that the increase of CA observed in this work for silicon dioxide surfaces may be a consequence of the exposure of ethoxy groups, which may result from incomplete hydrolysis or establishment of hydrogen bonds between the amine group of APTES and the hydroxyl groups from SiO_2.

As for **alumina** thin films, an increase in CA values was observed after exposure to APTES silane (CA reached $\simeq 90°$). Such as for SiO_2, this increase may be consequent of a major exposure of ethoxy groups after silanization. To understand the type of APTES-surface chemical bond, XPS analysis was performed, which results are discussed in section 3.2.1.

Chemical exposure of **gold** thin films ($CA_{gold;t0} \simeq 80°$) to a gas-phase of APTES resulted in a decrease of contact angle ($CA_{gold;t2} \simeq 45°$), which slowly increased with the increment of exposure time, reaching values of $\simeq 64°$ after 50 min. It is well explained in the literature that amine groups establish electrostatic bonds with gold by the free pair of electrons of the nitrogen atom, being the functionalization of hydrophilic surfaces with APTES for the immobilization of gold nanoparticles a common practice [28]. The presence of ethoxy groups on gold thin films following chemical exposure to APTES was expected due to the high amine-gold affinity [29]. However, the CA values observed may indicate that the reaction between APTES molecules and gold thin films was more complex than expected. Due to the hygroscopic character of APTES, the free ethoxy groups of attached APTES molecules (gold-amine interaction) may suffer hydrolysis (forming -OH groups) and covalently bond to free APTES molecules present in the vapor phase (forming Si-O-Si bonds), resulting in the exposure of amine and unreacted hydroxyl groups, which contribute to the increase of surface wettability. The slight increase of CA with the increment of time can also be explained by this reaction, as the increase of time leads to an increase of ethoxy groups at the surface that did not suffer hydrolysis (as the amount of water in the system is limited to the atmosphere and surface).

3.2.1 XPS analysis of alumina thin films

A sample of alumina thin film exposed to APTES by RT-CVD for 30 min and an untreated alumina substrate were analysed by XPS. Samples were analysed at take-off angle (TOA) 0° and 60° (angle with the normal to the surface). C 1s, Al 2p, O 1s, N 1s and Si 2p photo-electrons were acquired in detail. The elements which confirm undoubtedly the presence of APTES are the silicon (Si) and nitrogen (N), presented in fig. 8 and fig. 9, respectively.

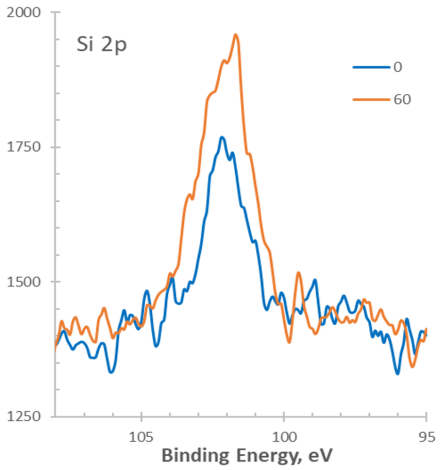

Figure 8: Si 2p XPS regions of Al_2O_3/APTES.

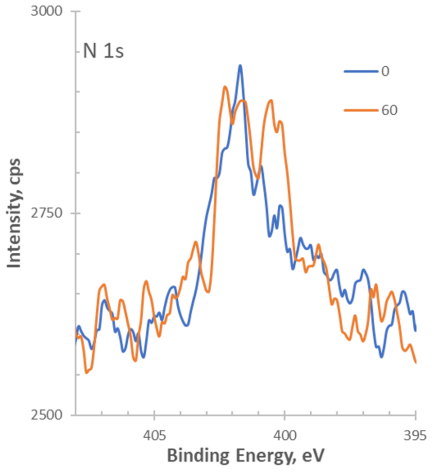

Figure 9: N 1s XPS regions of Al_2O_3/APTES.

A Si peak was observed in the alumina surface functionalized with APTES at 101.8 ± 0.1 eV, typical of siloxanes (Si-O-Si). Additionally, two nitrogen peaks were observed: at 400.4 ± 0.2 eV and 401.9 ± 0.2 eV. The first is assignable to an amine nitrogen while the second is assigned to a nitrogen with a decreased electronic density, possibly a N-O bond [30]. The quantitative analyses of spectra shows that Si 2p signal increases more than N 1s signal: N 1s/Si 2p(0°) = 0.90 and N 1s/Si 2p(60°) = 0.59. These values are compatible with the nitrogen being, in average, more buried than the silicon. The binding energy values indicate that a bond between the amine moiety of APTES and the hydroxyl groups of alumina was established, possibly through an hydrogen-bond.

3.3. *Textured Silicon Dioxide*

Results presented in fig.10 and fig. 11 demonstrate that implementation of deterministic roughness decreased the surface wettability of SiO_2 thin films, as CA measurements surpassed 90°.

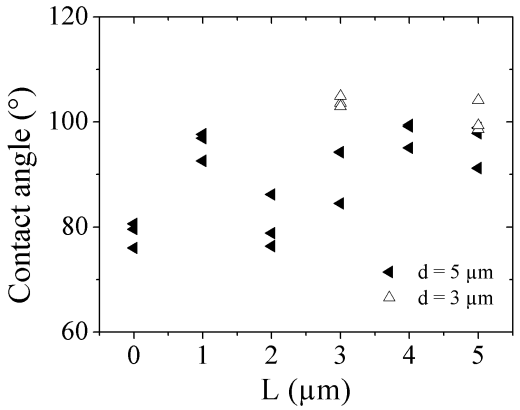

Figure 10: CA measurements of DI water droplets in contact with structures of increasing size.

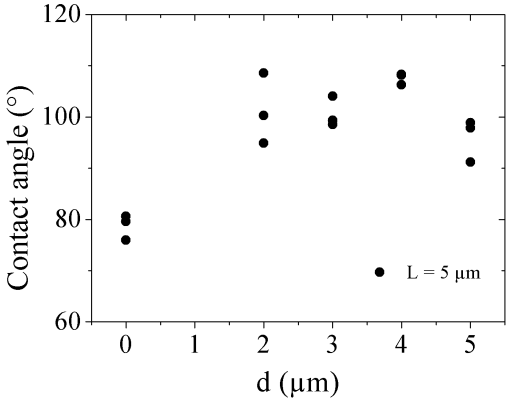

Figure 11: CA measurements of DI water droplets in contact with structures of increasing spacing.

Variation of structure size L (with fixed d of 5 μm) and spacing d (with fixed L of 5 μm) lead to an increase of CA values of 35 % and 21.2 %, respectively. An increase of structure size (fig. 10) lead to a decrease of surface wettability. However, it seems that the decrease of surface energy is more prominent for spacing (d) between 2 to 4 μm (fig.

11), possibly indicating that this parameter has a higher impact on SWM. This results are compatible with the results obtained by Fürstner *et al* [31], where the design of square structures of varying size (1-2 μm), spacing (1-5 μm) and heigh (1-4 μm) increased silicon wettability up to $\simeq 155°$. The authors observed that the increase of spacing lead to a decrease in CA, while an increase in structure size of 1 μm lead to a slight decrease in surface wettability.

The increase of contact angle or the decrease in surface wettability can be explained by the Cassie-Baxter (CB) model (eq. 3), where the increment in surface roughness leads to decrease of surface energy (or decrease in surface wettability), by the presence of air trapped between the structures.

The stability of the CB state depends on the vertical force (F) that actuates on a drop on top of a crevice (eq. 4), where ΔP is the Laplace pressure ($\Delta P = P_{liquid}$ - P_{air}) and A_{aw} is the horizontal projection area:

$$F = \Delta P * A_{aw} \tag{4}$$

Except for L=2;d=5 structures (fig. 10), the weight of 3 μL DI water droplets was not sufficient to create a high enough hydraulic pressure (P_{liquid}) to surpass the liquid-air energy barrier, thus inhibiting the wetting of the walls of the microfabricated structures.

4. Conclusions

SWM depends on several parameters: chemical layer of the substrate, silane hydrophobic/hydrophilic potential, presence of water, temperature, pressure and surface topography. Silanization with HMDS, FDTS and APTES by RT-CVD showed promising results, specially in hydroxyl-containing substrates where a covalent silane-surface bond was formed. For these substrates, a threshold of silanization was obtained earlier with FDTS and APTES (between 2 to 10 min of activation), which may be justified by their high hydrophobic potential. It was also observed a major preference of APTES molecules to establish amine-hydroxyl hydrogen bonds, instead of a covalent ethoxy-hydroxyl bond, described in the literature for liquid-phase silanization. This conclusion was reinforced by XPS analysis of alumina thin films, where the nitrogen seemed to be buried under silicon atoms, possibly attached to the surface by hydrogen bonds. Ultimately, RT-CVD revealed to be a promising method for chemical SWM, discarding the need for high temperature conditions (unlike typical CVD) for a successful silanization.

The design of square structures with varying size (1-5 μm) and spacing (2-5 μm) in SiO_2 thin films resulted in a hydrophobic behavior (CA>90°), which may be explained by the Cassie-Baxter model. Spacing between the square pillars seemed to have a higher impact on surface wettability, comparing to structure size, specially for 2 to 4 μm. Comparing the CA values of DI water droplets on SiO_2 thin films following chemical functionalization and implementation of deterministic roughness, the values obtained are quite similar (CA between 100° to 110°). This indicates that both techniques are useful to turn SiO_2 thin films hydrophobic, which can have many applications in biology and biomedicine, such as studies of cell behavior consequent of contact with certain chemical groups or specific topographies. These approaches are thus seen as straightforward, cost-effective and easily replicable methods to effectively tailor surface wettability of substrates also attractive in industrial context.

Acknowledgements

I would like to thank Professor Ana Maria Botelho do Rego and Dr.ª Ana Maria Ferraria from Centro de Quimica-Fsica Molecular (CQFM) of Instituto Superio Tecnico for the XPS analysis of thin films. I would also like to thank the personnel of INESC MN for the help in the processes of thin film deposition, etching and photolitography. INESC-MN acknowledges Fundação para a Ciência e a Tecnologia (FCT) funding through the Instituto de Nanociência e Nanotecnologia (IN) Associated Laboratory and projects POCI-01-0145-FEDER-016623 and PTDC/CTM-NAN/3146/2014, financed by FEDER (Quadro Portugal 2020) and FCT. This project has received funding from National Funds through FCT under the project PTDC-FIS-PLA-31055-2017.

References

[1] Tehranirokh M., Kouzani A., Francis P., and Kanwar J. *Biomicrofluidics*, 7(5):051502, 2013. doi:10.1063/1.4826935.

[2] Silverio V., Canane P., and de Freitas S.C. *Colloids and Surfaces A: Physicochemical and Engineering Aspects*, 2019. doi: 10.1016/j.colsurfa.2019.03.032.

[3] Nguyen A. T., Sathe S. R., and Yim E. K .F. *Journal of Physics: Condensed Matter*, 28(18):183001, 2016. doi: 10.1088/0953-8984/28/18/183001.

[4] Streicher R., Schmidt M., and Silvana F. *Future Medicine*, 2(6):861–874, 2007. doi: 10.2217/17435889.2.6.861.

[5] Oliver R. W. A. volume 872. Oxford University Press on Demand, 1998.

[6] Zhan S., Pan Y., Z. F. Gao, Lou X., and F. Xia. *Trends in Analytical Chemistry*, 108:183–194, 2018. doi: 10.1016/j.trac.2018.09.001.

[7] Wassmann T., Kreis S., Behr M., and Buergers R. *International journal of implant dentistry*, 3(1):32, 2017. doi: 10.1186/s40729-017-0093-3.

[8] Ulman A:. *Chemical reviews*, 96(4):1533–1554, 1996. doi: 10.1021/cr9502357.

[9] Shuai H-H., Yang C-Y., Hans I, . Harn C, York R. L., Liao T-C., Chen W-S., Yeh J. A., and Cheng C-M. *Chemical Science*, 4(8):3058–3067, 2013. doi: 10.1039/C3SC50533B.

[10] Kwon D., H. Yoo, Lee H., and Jeon S. *Sensors and Actuators B: Chemical*, 255:552–556, 2018. doi: 10.1016/j.snb.2017.08.105.

[11] Den Besten C., Van Hal R. E. G., Munoz J., and Bergveld P. In *Proceedings IEEE Micro Electro Mechanical Systems*, pages 104–109, 1992. doi: 10.1109/MEMSYS.1992.187699.

[12] Zubayda S Saifaldeen, Khedir R Khedir, Merve T Camci, Ahmet Ucar, Sefik Suzer, and Tansel Karabacak. *Applied Surface Science*, 379:55–65, 2016. doi: 10.1016/j.apsusc.2016.04.050.

[13] Acres R. G., Ellis A. V., Alvino J., Lenahan C. E., Khodakov D. A., Metha G. F., and Andersson G. G. *The Journal of Physical Chemistry C*, 116(10):6289–6297, 2012.

[14] H Gert, Nolan Foley, Darin Zwaan, Bart J Kooi, and George Palasantzas. *RSC Advances*, 5(36):28696–28702, 2015. doi: 10.1039/c5ra02348c.

[15] Liu Y., Moevius L., Xu X., Qian T., Yeomans J., and Wang Z. *Nature Physics*, 10(7):515, 2014. doi: 10.1038/nphys2980.

[16] Zhang Y. 2007. doi: 10.31274/rtd-180813-17133.

[17] Stalder A., Melchior T., Müller M., Sage D., Blu T., and Unser M. *Colloids and Surfaces A: Physicochemical and Engineering Aspects*, 364(1-3):72–81, 2010. doi: 10.1016/j.colsurfa.2010.04.040.

[18] Zisman W. A. *Advan. Chem. Ser.*, 43:1–51, 1964. doi: 10.1021/ba-1964-0043.ch001.

[19] Bekir S Yilbas, Haider Ali, Muhammad R Yousaf, and Abdullah Al-Sharafi. 2.25 hydrophobic materials. 2.

[20] Hair M. L. *Journal of Non-Crystalline Solids*, 19:299–309, 1975. doi: 10.1016/0022-3093(75)90095-2,.

[21] Lima R. S., P. Leão, Piazzetta M., Monteiro A. M., Shiroma L. Y., Gobbi A. L., and Carrilho E. *Scientific reports*, 5:13276, 2015. doi: 10.1038/srep13276.

[22] Zhuang Y. X., Hansen O., Knieling T., Wang C., Rombach P., Lang W., Benecke W., Kehlenbeck M., and Koblitz J. *Journal of Microelectromechanical Systems*, 16(6):1451–1460, 2007. doi: 10.1109/JMEMS.2007.904342.

[23] Tasaltin N., Sanli D., Jonáš A., Kiraz A., and Erkey C. *Nanoscale research letters*, 6(1):487, 2011. doi: 10.1186/1556-276X-6-487.

[24] Zhang L., Kuramoto N., Azuma Y., Kurokawa A., and Fujii K. *IEEE Transactions on Instrumentation and Measurement*, 66(6):1297–1303, 2016. doi: 10.1109/TIM.2016.2634678.

[25] Smith T. *Journal of Colloid and Interface Science*, 75(1):51–55, 1980. doi: 10.1016/0021-9797(80)90348-3.

[26] Chaigneau M., Picardi G., and Ossikovski R. *Surface Science*, 604(7-8):701–705, 2010. doi: 10.1016/j.susc.2010.01.018.

[27] Kyaw H., Al-Harthi S. H., Sellai A., and Dutta J. *Beilstein journal of nanotechnology*, 6(1):2345–2353, 2015. doi: 10.3762/bjnano.6.242.

[28] Grabar K. C., Hommer R. G., Freeman an M. B., and Natan M. J. *Analytical chemistry*, 67(4):735–743, 1995. doi: 10.1021/ac00100a008.

[29] Connolly D., Twamley B., and Paull B. *Chemical Communications*, 46(12):2109–2111, 2010. doi: 10.1039/B924152C.

[30] Beamson G. and Briggs D. High resolution xps of organic polymers. *Journal of Chemical Education*, 1992. doi: 10.1021/ed070pA25.5.

[31] Fürstner R., Barthlott W., Neinhuis C., and Walzel P. *Langmuir*, 21(3):956–961, 2005. doi: 10.1021/la0401011.